

Field-gradient-induced second-harmonic generation in magnetized vacuum

A. E. Kaplan¹ and Y. J. Ding²¹*Department of Electrical and Computer Engineering, Johns Hopkins University, Baltimore, Maryland 21218*²*Department of Physics, University of Arkansas, Fayetteville, Arkansas 72701*

(Received 19 January 2000; published 12 September 2000)

The photon-photon scattering in vacuum can give rise to the second-harmonic generation of intense laser radiation in a dc magnetic field in the “box” diagram approximation of quantum electrodynamics if the symmetry of interaction is broken by *modulation or/and nonuniformity* of optical wave +dc field system in time or/and space. Specific examples considered here are: an optical *pulse* plane wave or a Gaussian laser beam propagating in uniform or nonuniform dc fields.

PACS number(s): 42.65.Ky, 12.20.-m

I. INTRODUCTION

Photon-photon scattering [1,2] is perhaps one of the most fundamental quantum electrodynamics (QED) processes, which may also result in nonlinear optical effects in vacuum such as the birefringence of the refractive index seen by a probe field under the action of either a dc magnetic (or electric) field [3] or intense laser pumping [4], multiwave mixing [5], and merging of two photons into one (i.e., sum frequency generation) [6] under the action of a dc field. All of these effects are based on the lowest order, so called “box” diagram approximation, Fig. 1. (It was also proposed that using hexagonal diagram, high-order harmonics [7], and second-order subharmonic, a so-called photon splitting [3,8], can be generated with a dc magnetic field.) If observed, these effects may provide a fundamental optical test of QED.

From any realistic point of view the only hope to attain observable effects in the laboratory is to use lowest-order processes (i.e., those due to the box diagram); yet the required optical fields are still enormously high and not presently available. It has also been apparent that a dc field (either electric or magnetic) may greatly assist the interaction, which have attracted much attention [3–8]. One of the most interesting and fundamental are dc field-assisted processes: the merging of two photons into one, e.g., the second-harmonic generation (SHG) Fig. 1 [3,8] (see also [9,10]), and photon “splitting” [6,3,8], (see also [11])—in essence, a parametric process—in the presence of a dc field. However, these processes have been the subject of a long persisting controversy, with the work [3,6,8] maintaining (correctly, see below) that these effects vanish in the box approximation (and under condition of cw wave and uniform and constant dc field, which is an important point in the context of this paper), whereas the work [9–11] suggested (erroneously, see Refs. [3], [8b], and [12]) nonvanishing effect for the same approximation and conditions. The previous works on the subject have been reviewed in [12] with a conclusion that none of them were fully correct although the results [12] are much closer to those of Refs. [3], [6], [8] [the results of [12] suggests the box diagram contribution for the plane wave is nonzero, yet smaller than that from the next order, hexagonal, diagram]. Our recent proposal [13] of laser-induced SHG in vacuum in the presence of a dc magnetic field has been criticized from QED [14] and phenomenological [15]

points of view (see also earlier work [6]), pointing out that SHG in configuration [13] should vanish. While being in agreement with the major point of Refs. [14,15] that SHG due to the box diagram vanishes for a cw plane wave and uniform dc field (which was also the main case considered earlier [3–15]), our reply [16] and later consideration [17] suggested, however, that the nonvanishing effect may result from the spatial *nonuniformity* of the field.

Hence, the fundamental question arises whether the vanishing contribution of the box diagram is due to fundamental laws of QED, or only due to the conventionally (and thus unfavorably) chosen configuration: plane monochromatic (cw) optical wave+uniform dc field. In this paper, we show that the nonvanishing contribution of the box diagram can result from the nonuniformity (or gradient) of *any* component of the *entire* field system (both the laser and dc magnetic fields) in *space* or/and *time* (Sec. II). In particular, we consider a plane wave modulated in *time* by a pulse with an arbitrary profile and finite duration (Sec. III), and a cw Gaussian (i.e., spatially *inhomogeneous*) laser beam in a magnetic field with an arbitrary spatial distribution (Sec. IV), in particular in both *uniform* (Sec. V) and *nonuniform* fields—magnetic dipole and quadrupole (Sec. VI). We demonstrate that the nonvanishing SHG in the lowest (i.e., box) approximation exists in all these configurations. The most important fact is that the SHG effect (i) exists in the approximation in which the plane-wave SHG vanishes completely, and (ii) that it is of the expected order of magnitude; for example, for a Gaussian laser field with maximum amplitude E_1 in the focal plane in a uniform dc magnetic field B_0 , the efficiency of SHG conversion w_{SHG} is

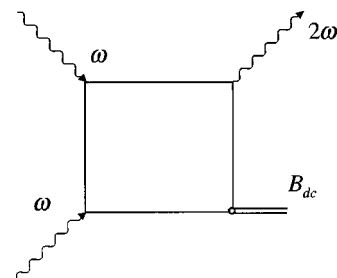


FIG. 1. Fourth-order (“box”) Feynman diagram for photon-photon scattering in a dc field resulting in second-harmonic generation (SHG).

$$w_{\text{SHG}} = (\alpha/45)^2 O[(E_1 B_0 / B_{\text{cr}}^2)^2], \quad (1.1)$$

[see Eq. (5.7) below], where B_{cr} is the QED critical field (see below), and $\alpha = e^2/\hbar c = 1/137$ is the fine structure constant; the advent of laser and magnet technology may make the observation of vacuum SHG feasible in the foreseeable future (Sec. VII). Our interpretation of field-gradient-induced SHG in vacuum relates the field nonuniformity to momentum transfer between photons and the dc field (Sec. VII). The total number of SHG photons in such a system is many orders of magnitude higher than that due to the next, hexagonal diagram contribution, such that SHG appears to be truly of the ‘‘box diagram’’ nature (Sec. VII).

II. SECOND-ORDER OPTICAL NONLINEARITY IN A dc MAGNETIC FIELD

The Heisenberg-Euler Lagrangian [1,2] for PPS can be written as

$$L = L_2 + L_4 + L_6 + \dots,$$

where $L_2 = (E^2 - B^2)/2$ is a linear term, and

$$L_4 = (\chi/2)(a^2 + b^2); \quad (a \equiv E^2 - B^2; b \equiv \vec{E} \cdot \vec{B}) \quad (2.1)$$

is the first nonlinear term; it corresponds to the box Feynman diagram. Here

$$\chi = \alpha/45\pi B_{\text{cr}}^2 = 2.6 \times 10^{-24} \text{ tesla}^{-2}$$

is a nonlinear interaction constant and

$$B_{\text{cr}} \equiv m_0^2 c^3 / e \hbar = 4.4 \times 10^9 \text{ tesla}$$

is the QED critical field. L_6 corresponds to the hexagonal Feynman diagram (see below, Sec. VII), etc. Using the action for the first two terms, $\int (L_2 + L_4) d^4x$, and taking the variation with respect to the four-vector potential, the macroscopic equations in the form of classical Maxwell's equations are obtained as [1,2,6,18]

$$\vec{\nabla} \cdot \vec{B} = 0, \quad \vec{\nabla} \cdot \vec{D} = 0, \quad (2.2)$$

$$\vec{\nabla} \times \vec{E} + \partial \vec{B} / c \partial t = 0, \quad \vec{\nabla} \times \vec{H} - \partial \vec{D} / c \partial t = 0,$$

with the constitutive relations [1,2,18] between the electric displacement \vec{D} and magnetic field \vec{H} , and electric field \vec{E} and magnetic induction \vec{B} being:

$$\vec{D} = \vec{E} + \vec{D}^{\text{NL}}, \quad \vec{H} = \vec{B} - \vec{H}^{\text{NL}}, \quad (2.3)$$

where

$$\vec{D}^{\text{NL}} = \partial L_4 / \partial \vec{E} = \chi(2a\vec{E} + 7b\vec{B}), \quad (2.4a)$$

$$\vec{H}^{\text{NL}} = \partial L_4 / \partial \vec{B} = \chi(-2a\vec{B} + 7b\vec{E}). \quad (2.4b)$$

These equations are valid for $|E|, |B| \ll B_{\text{cr}}$ and $\lambda \gg \bar{\lambda}_C$, [18,19], where λ is the field wavelength and $\bar{\lambda}_C = \hbar/m_0 c = 3.862 \times 10^{-3} \text{ \AA}$ is the Compton wavelength of the electron.

A cw plane wave does not exhibit any nonlinear effects, since due to its properties,

$$E^2 = B^2, \quad \vec{E} \cdot \vec{B} = 0 \quad (\text{i.e., } a = b = 0),$$

the nonlinearity, Eq. (2.4), vanishes. This ‘‘degeneracy’’ of the *third-order* nonlinearity may be broken by the field nonuniformity that can give rise to *second-order* nonlinear *optical* effects in the presence of a strong *static* field. If an unperturbed fundamental wave, \vec{E}_1 and \vec{B}_1 , propagates in vacuum in the presence of a dc magnetic field, \vec{B}_{dc} , Eq. (2.4) can be rewritten as

$$\vec{D}^{\text{NL}} = \chi(-2B_{\text{dc}}^2 \vec{E}_1 + 7b_E \vec{B}_{\text{dc}}) + \vec{D}^{(2)}, \quad (2.5a)$$

$$\vec{H}^{\text{NL}} = 2\chi B_{\text{dc}}^2 \vec{B}_{\text{dc}} + 2\chi(B_{\text{dc}}^2 \vec{B}_1 + 2b_B \vec{B}_{\text{dc}} + \vec{H}^{(2)}), \quad (2.5b)$$

where $b_B = \vec{B}_1 \cdot \vec{B}_{\text{dc}}$, $b_E = \vec{E}_1 \cdot \vec{B}_{\text{dc}}$, and the only terms that may give rise to SHG are

$$\vec{D}^{(2)} = \chi(4b_B \vec{E}_1 - 7b_E \vec{B}_1); \quad \vec{H}^{(2)} = \chi(4b_B \vec{B}_1 + 7b_E \vec{E}_1). \quad (2.6)$$

Suppose now that the unperturbed fundamental light beam at the frequency ω_1 is a quasiplane and/or quasi-cw wave with the wave vector $\vec{k}_1 = \vec{q}_1 k_1$, $k_1 = \omega_1 / c$, $q_1 = 1$, such that

$$\vec{E}_1 = \vec{p}_1 u_1(\vec{r}, \Psi) \cdot e^{-i\psi}, \quad \vec{B}_1 \approx \vec{q}_1 \times \vec{E}_1, \quad \vec{p}_1 \cdot \vec{q}_1 = 0, \quad (2.7)$$

where \vec{p}_1 is a polarization vector ($|\vec{p}_1| = 1$), $\psi = \omega_1 t - \vec{r} \cdot \vec{k}_{10}$ is a retarded coordinate, and u_1 is a ‘‘slow’’ envelope, whose variations in space r and in ψ are much slower than $e^{-i\psi}$ (for a cw plane wave, $\vec{p}_1 u_1 = \text{const}$). Here $\vec{k}_{10} = k_1 \vec{q}_{10}$, where \vec{q}_{10} is a unity vector along the main axis of the beam propagation. Using Eqs. (2.6) and (2.7), we find that

$$\vec{D}^{(2)} \cdot \vec{H}^{(2)} = 0; \quad |\vec{D}^{(2)}| = |\vec{H}^{(2)}|; \quad \vec{H}^{(2)} \approx -\vec{q}_1 \times \vec{D}^{(2)}. \quad (2.8)$$

The SHG wave equations can then be obtained from Eqs. (2.2) and (2.4) as

$$\nabla \times \vec{E}_2 + (1/c) \partial \vec{B}_2 / \partial t = 0, \quad (2.9)$$

$$\nabla \times \vec{B}_2 - (1/c) \partial \vec{E}_2 / \partial t = \vec{F} \cdot \chi e^{-2i\psi},$$

where

$$\vec{F} = \chi^{-1} [(1/c) \partial \vec{D}^{(2)} / \partial t + \nabla \times \vec{H}^{(2)}] \cdot e^{2i\psi} \quad (2.10)$$

is a slow envelope of nonlinear driving term (or source). Using Eqs. (2.6) and (2.7), we find

$$\vec{F} = k_1 \partial \vec{f} / \partial \psi - \nabla \times [\vec{q}_1 \times \vec{f}] + 2ik_1 \vec{\Delta} q \times [\vec{q}_1 \times \vec{f}], \quad (2.11)$$

where $\vec{\Delta}_q = \vec{q}_1 - \vec{q}_{1_0}$ and

$$\vec{f} = \vec{p}_2 \cdot u_1^2 \mathbf{B}_{dc}, \quad (2.12')$$

$$\vec{p}_2 = -4\vec{p}_1 \cdot ([\vec{q}_1 \times \vec{p}_1] \cdot \vec{e}_{dc} + 7(\vec{p}_1 \cdot \vec{e}_{dc})[\vec{q}_1 \times \vec{p}_1]), \quad (2.12'')$$

with \vec{p}_1 , \vec{q}_1 , and $\vec{e}_{dc} = \vec{B}_{dc}/B_{dc}$ being the unity vectors of the wave polarization, the wave direction of propagation, and the dc magnetic field, respectively. In Eq. (2.12), \vec{p}_2 is a (non-unity in general) SH polarization vector. Because of the spatial anisotropy imposed by a dc magnetic field, SHG depends upon the polarization of laser fundamental wave; Eq. (2.12) reflects induced birefringence of the nonlinear interaction. If the fundamental wave propagates along the dc magnetic field \vec{B}_0 , then $\vec{D}^{(2)} = 0$, $\vec{H}^{(2)} = 0$ [Eq. (2.4)], and nonlinear effects vanish identically. The strongest interaction occurs when the light propagates *normally* to \vec{B}_0 and is polarized parallel to \vec{B}_0 , in which case

$$\vec{p}_1 = \vec{e}_{dc}, \quad \text{and} \quad \vec{p}_2 = 7[\vec{q}_1 \times \vec{p}_1], \quad (2.13)$$

i.e., here the SH polarization vector \vec{p}_2 is *normal* to the fundamental polarization vector \vec{p}_1 . This is the manifestation of birefringence; note that when the fundamental light is polarized (and propagates) *normally* to the magnetic field, the SH polarization coincides with that of the fundamental radiation:

$$\text{if } \vec{p}_1 \parallel \vec{e}_{dc} \text{ \& } \vec{q}_1 \parallel \vec{e}_{dc}, \text{ then } \vec{p}_2 = 4\vec{p}_1. \quad (2.14)$$

The first term in the right-hand side of Eq. (2.11) is due to the time dependence of the dc field and the intensity of the fundamental wave, whereas the second and third terms are due to spatial nonuniformity of the wave intensity and phase, respectively. Equation (2.11) clearly indicates that the driver \vec{F} (and therefore, SHG itself) vanishes (consistently with [14,15,6]), if the radiation is a cw plane wave and the dc field is uniform and constant, since in such a case $\partial/\partial\psi = 0$, $\Delta q = 0$, and $\nabla = 0$. Thus, the nonvanishing effect may be expected only if the field system varies in space and/or time.

The evolution of an unperturbed fundamental wave envelope u_1 of a diffracting light beam in a vacuum is governed by a so-called paraxial wave equation that approximates Eqs. (2.2) under the condition $\partial^2 E_1 / \partial y^2 \ll k_1 \partial E_1 / \partial y$:

$$2ik_1 \partial u_1 / \partial y + \Delta_{\perp} u_1 = 0, \quad (2.15)$$

where we assumed the laser beam to propagate along the y axis (i.e., $\vec{q}_{1_0} = \hat{e}_y$); $\Delta_{\perp} = \partial^2 / \partial x^2 + \partial^2 / \partial z^2$ is a ‘‘transverse’’ Laplacian. Since in this approximation, vacuum is dispersionless, no time derivative (or $\partial/\partial\psi$) enters this equation, i.e., the temporal (or ψ) modulation of the envelope u_1 remains intact as the wave propagates. Using the same approximation for SHG, assuming $\vec{E}_2 = \vec{u}_2(\vec{r}, \psi) e^{-2i\psi}$ and slow variation of \vec{B}_{dc} in time/space, we obtain a paraxial equation for an SHG slow envelope \vec{u}_2 as

$$4ik_1 \partial \vec{u}_2 / \partial y + \Delta_{\perp} \vec{u}_2 = -2ik_1 \chi \vec{F}. \quad (2.16)$$

III. PULSE PROPAGATION IN AN UNIFORM dc MAGNETIC FIELD

Consider first the perhaps simplest and fundamental example of a *pulse* plane wave propagating in a *uniform dc* magnetic field ($\vec{B}_{dc} = B_0 \hat{e}_z$; $\vec{e}_{dc} = \hat{e}_z$) normal to the wave propagation axis, y , i.e., $\vec{q}_1 = \hat{e}_y$. Suppose that the amplitude (and/or phase) of fundamental plane wave ($\Delta_{\perp} u_1 = 0$) is *arbitrarily* modulated in time with a (complex) envelope $u_1(\psi)$ and let θ_1 be the angle between \vec{p}_1 and \vec{B}_{dc} [i.e., $\vec{p}_1 = (\vec{p}_1)_0 \equiv \sin \theta_1 \hat{e}_x + \cos \theta_1 \hat{e}_z$]. The SHG driver, Eq. (2.11), is then reduced to:

$$\vec{F} = k_1 \partial \vec{f} / \partial \psi = k_1 B_0 \vec{p}_2 d[u_1^2(\psi)]/d\psi, \quad (3.1)$$

where

$$\vec{p}_2 = (4 + 3 \cos^2 \theta_1) \hat{e}_x - 3 \sin \theta_1 \cos \theta_1 \hat{e}_z. \quad (3.2)$$

(Note again that for $\theta_1 = 0$, i.e., when $\vec{p}_1 \parallel \vec{B}_0$, then $\vec{p}_2 = 7\hat{e}_x$, and $\vec{p}_2 \parallel \vec{p}_1$. When $\theta_1 = \pi/2$, i.e., if $\vec{p}_1 \perp \vec{B}_0$, we have $\vec{p}_2 = 4\vec{p}_1$.) Thus, SHG may occur only if the fundamental wave envelope is *time* (or ψ) *dependent*. The plane-wave ($\Delta_{\perp} u_2 = 0$) solution of Eq. (2.16) with a driver, Eq. (3.1), is found as

$$\vec{u}_2(\psi, y) = -(\chi/2) k_1 B_0 \vec{p}_2 y d[u_1^2(\psi)]/d\psi, \quad (3.3)$$

assuming that the field B_0 is ‘‘turned on’’ at $y=0$. Equation (3.3) demonstrates the same dependence on the *distance* of interaction ($u_2 \propto y$) as for SHG in a ‘‘classical’’ nonlinear medium with ideal phase matching, with the significant difference being that SHG is proportional now to the time derivative of the driving envelope. The use of very broad spectrum radiation can further enhance the SHG effect.

The SHG energy flux at each point in the y axis is

$$\mathcal{E}_{\text{SHG}}(y) = (c/2) \int_{-\infty}^{\infty} |u_2|^2 dt.$$

Assuming a Gaussian temporal intensity envelope of the fundamental wave,

$$u_1^2 = E_1^2 \exp(-t^2/t_p^2),$$

where $2t_p$ is total pulse length, we obtain from Eq. (3.3) that

$$\mathcal{E}_{\text{SHG}}(y) = (p_2^2/8ct_p) \sqrt{\pi/2} (\chi B_0 E_1^2 y)^2. \quad (3.4)$$

(For $\theta_1 = 0$, $|p_2| = 7$, while for $\theta_1 = \pi/2$, $|p_2| = 4$.) Since the energy flux at the fundamental frequency is $\mathcal{E}_1 = (c/2) \int_{-\infty}^{\infty} |u_1|^2 dt$, we obtain the efficiency of the SHG conversion as:

$$\frac{\mathcal{E}_{\text{SHG}}(y)}{\mathcal{E}_1} = \frac{1}{\sqrt{2}} \left(\frac{\alpha p_2 B_0 E_1 y}{90\pi B_{\text{cr}}^2 ct_p} \right)^2. \quad (3.5)$$

IV. TWO-DIMENSIONAL (2D) cw GAUSSIAN BEAM IN A dc MAGNETIC FIELD

Considering now *spatial* nonuniformity of nonplanar (in particular, Gaussian) wave, we assume a cw wave (it is clear however that a combined time/space nonuniformity may significantly enhance the nonlinear interaction), such that in Eq. (2.11), $\partial/\partial\psi=0$. The calculations of the beam propagation for SHG in the general case become tedious, and to make them more traceable, we consider here the probably simplest case of spatially nonuniform problem: the propagation of a 2D Gaussian beam (or so called *slab* beam), in which case it is assumed uniform along only one direction (say in the x axis, so that $\partial/\partial x=0$), and having a Gaussian profile in the other direction (say the z axis) normal to the direction of the propagation (the y axis). In this case the transverse Laplacian in Eqs. (2.15) and (2.16) is $\Delta_{\perp}=\partial^2/\partial z^2$. To maximize the interaction, we assume that the dc magnetic field \vec{B}_{dc} , is normal (or almost normal) to the direction of the wave propagation (such that $|B_z|\gg|B_y|$, and $B_x=0$), and the fundamental wave is polarized normally to \vec{B}_{dc} , with

$$\vec{E}_1=\vec{p}_1 u_1 e^{-i\psi},$$

where now $\psi=\omega_1 t-k_1 y$ and $\vec{p}_1=\hat{e}_x$. A fundamental solution of Eq. (2.15) in such a case is a 2D Gaussian beam:

$$u_1=E_1 G(y,z); \quad G=\sqrt{Y(y)} \exp[-Y(y)z^2/2z_0^2];$$

$$Y(y)\equiv(1+iy/y_d)^{-1}, \quad (4.1)$$

where $E_1=\text{const}$ is its maximum amplitude (i.e., at the waist), a function G describes a Gaussian transverse amplitude (and phase) profile and its spatial evolution due to diffraction. $Y(y)$ is a ‘‘diffraction’’ factor, z_0 is the minimum size of the beam (at the waist, $y=0$), and

$$y_d=z_0^2 k_1=z_0/\phi_d, \quad \phi_d=(k_1 z_0)^{-1}\ll 1, \quad (4.2)$$

where y_d is the Rayleigh parameter (diffraction length) of the beam, with ϕ_d being a diffraction angle. Note that the size of the Gaussian beam is found as

$$z_G(y)=z_0\sqrt{1+(y/y_d)^2} \quad \text{or} \quad z_G/y_d=\phi_d\sqrt{1+(y/y_d)^2}. \quad (4.1')$$

From Eq. (2.12) we obtain the SHG polarization vector

$$\vec{p}_2=4\vec{q}_1\times\vec{e}_{dc}; \quad (\vec{p}_2\cdot\vec{q}_1=0; \quad \vec{p}_2\parallel\vec{p}_1). \quad (4.3)$$

Here the the components $q_j\equiv\vec{q}_1\cdot\vec{e}_j$ of the propagation vector \vec{q}_1 are: $q_x=0$, $q_y=\cos\phi$, $q_z=\sin\phi$, where

$$\phi=\frac{z y}{(y^2+y_d^2)}=\phi_d\left[\frac{z}{z_0}\right]\left[\frac{y}{y_d}\right]|Y(y)|^2\ll 1 \quad (4.4)$$

is the angle of the energy propagation (normal to the phase front of the fundamental wave) at each point (y,z) . Equation (2.11) yields

$$\vec{F}=\vec{p}_1[\text{div}(\vec{q}_1 f p)-4ik_1 f p \sin^2(\phi/2)], \quad (4.5)$$

where $f=4u_1^2 B_{dc}$, $\vec{q}_1=\hat{e}_y \cos\phi+\hat{e}_z \sin\phi$, and $p=(\hat{e}_{dc})_z \cos\phi-(\hat{e}_{dc})_y \sin\phi$. Recalling that

$$\phi\ll 1, \quad (\hat{e}_{dc})_y\ll(\hat{e}_{dc})_z, \quad \text{and} \quad z_0\ll z_B,$$

(where z_B is the z -spatial scale of the dc magnetic field when it is inhomogeneous, see below), and thus $1-p=O(\phi_d\cdot z_0/z_B)\ll\ll$, we find

$$4ik_1 f p \sin^2(\phi/2)\approx ik_1 f \phi^2, \quad (4.6')$$

where we neglected terms $o(\phi_d^2)$, and

$$\text{div}(\vec{q}_1 f p)=\partial(\phi f)/\partial z+\partial f/\partial y, \quad (4.6'')$$

or, since we assumed that $z_0\ll z_B$, i.e., that the dc magnetic field $B_{dc}(y,z)$ is changing much slower across the optical beam (i.e., as function of z) than the light intensity $u_1^2(y,z)$,

$$\text{div}(\vec{q}_1 f p)=4\left[B_{dc}\frac{\partial(\phi u_1^2)}{\partial z}+\frac{\partial(u_1^2 B_{dc})}{\partial y}\right]. \quad (4.7)$$

Substituting Eqs. (4.6) and (4.7) into Eq. (4.5), and using Eq. (4.1), $u_1^2=E_1^2 Y(y)\exp[-Y(y)z^2/z_0^2]$, we obtain finally:

$$\vec{F}=4\vec{p}_1 u_1^2\left[\frac{\partial B_{dc}}{\partial y}-i\left(\frac{B_{dc}}{y_d}\right)|Y(y)|^2\left(1-|Y|^2\frac{z^2}{z_0^2}\right)\right]. \quad (4.8)$$

Here, the first term in square brackets is due to the spatial nonuniformity of the dc field, whereas the rest of the expression is due to the inhomogeneity of the laser field. Note again that for the plane wave and uniform dc field, i.e., when $z_0\rightarrow\infty$, $y_d\rightarrow\infty$, and $dB_{dc}/dy=0$, the effect vanishes since then $\vec{F}\rightarrow 0$. A significant feature of the solution for the driver, Eq. (4.8), is that in addition to the expected component simply mimicking the (square of) the Gaussian profile of the fundamental wave (the terms in the brackets independent of z), it also has a term proportional to z^2 [the last term in Eq. (4.8)], which reflects the generation of a higher-order Gaussian component in the SHG beam. (For a 3D cylindrically symmetric beam [17] not considered here, the counterpart of such a mode would be a so called ‘‘doughnut’’ mode. It is worth noting that the doughnut SHG mode has been observed experimentally with ‘‘classic’’ SHG in gasses+plasmas [20], wherein the effect has also been attributed to the field gradient.)

Considering now SHG spatial dynamics with $\vec{u}_2=\vec{p}_1 u_2$ and $\partial u_2/\partial x=0$, and normalizing our variables as

$$\xi\equiv\frac{y}{y_d}; \quad \zeta\equiv\frac{z}{z_0}; \quad v\equiv\frac{u_2}{4\chi E_1^2 B_0}; \quad \beta\equiv\frac{B_{dc}}{B_0}, \quad (4.9)$$

where B_0 is maximal dc magnetic field, we reduce Eq. (2.16) to:

$$4i\frac{\partial v}{\partial \xi}+\frac{\partial^2 v}{\partial \xi^2}=-2Y(\xi)e^{-Y\zeta^2}\left[i\frac{\partial \beta}{\partial \xi}+\beta|Y|^2(1-|Y|^2\zeta^2)\right]. \quad (4.10)$$

The exact *driven* solution of this equation can be expressed in terms of combination of the fundamental (zeroth order) v_{f0} and second-order v_2 standard Gaussian modes:

$$v(\xi, \zeta) = v_{f0} + v_2 \\ = [g_{f0}(\xi) + g_2(\xi)(\zeta^2 - |2Y|^{-2})]Y(\xi)e^{-Y\xi^2}, \quad (4.11)$$

where $Y(\xi) = (1 + i\xi)^{-1}$, and the amplitudes $g_{f0}(\xi)$ and $g_2(\xi)$ of the respective modes are governed by the ordinary differential equations:

$$2ig'_{f0} + g_{f0}Y = -(i\beta' + 3\beta|Y|^2/4); \quad (4.12a)$$

$$2ig'_2 - 3g_2Y = \beta|Y|^4; \quad (4.12b)$$

where prime denotes $d/d\xi$. Note that a standard second-order mode in Eq. (4.11) is constructed in such a way (see the ‘‘bias’’ term, $|2Y|^{-2}$) as to secure the orthogonality of the modes, $\int_{-\infty}^{\infty} v_{f0} v_2^* d\zeta = 0$, at each point in ξ . With the zero driver (say, $\beta = 0$), the solution of Eq. (4.12) is:

$$g_{f0}(\xi) = C_{f0}Y^{-1/2}(\xi); \quad g_2(\xi) = C_2Y^{3/2}, \quad (4.13)$$

(where C_{f0} and C_2 are integration constants), which are expected amplitudes of the zeroth and second-order modes of a Gaussian beam in a linear vacuum; if no light at the frequency 2ω is incident upon the system at $\xi \rightarrow -\infty$, we naturally have $C_{f0} = C_2 = 0$. For the *driven* solution, one has to stipulate that the total SHG power vanishes at $\xi \rightarrow -\infty$. The total SHG power, W_{SHG} , per unity length in the x axis through the entire beam’s cross section normal to the axis of propagation y is

$$W_{\text{SHG}}(y) = (c/2) \int_{-\infty}^{\infty} |u_2(y, z)|^2 dz \\ = (c/2)(4\chi E_1^2 B_0)^2 z_0 \sqrt{\pi/2} P_{\text{SHG}}, \quad (4.14)$$

or

$$W_{\text{SHG}} = (4\xi W_1 B_0)^2 \sqrt{2/\pi} P_{\text{SHG}} / cz_0, \quad (4.15)$$

where

$$W_1 = (c/2) \int_{-\infty}^{\infty} |u_1|^2 dz = (c/2) E_1^2 z_0 \sqrt{\pi} \quad (4.16)$$

is the laser power (i.e., that of fundamental harmonic) per unity length in the x axis, and P_{SHG} is dimensionless normalized total SHG power:

$$P_{\text{SHG}}(\xi) = \sqrt{2/\pi} \int_{-\infty}^{\infty} |v|^2 d\zeta = P_{00} + P_{22}. \quad (4.17)$$

Here P_{00} and P_{22} are dimensionless normalized powers of zeroth and second-order modes, respectively, defined as

$$P_{jj}(\xi) = \sqrt{2/\pi} \int_{-\infty}^{\infty} |v_j(\xi, \zeta)|^2 d\zeta,$$

so that

$$P_{00} = |g_{f0}|^2 |Y|; \quad P_{22} = |g_2|^2 (2|Y|)^{-3}. \quad (4.18)$$

V. A GAUSSIAN BEAM IN AN UNIFORM dc MAGNETIC FIELD

Consider first the simplest case: the dc magnetic field is uniform, $\vec{B}_{\text{dc}} = B_0 \hat{e}_z = \text{const}$, and thus $\beta = \text{const} = 1$, $\beta' = 0$. Using a variable, $\Phi \equiv (\tan^{-1} \xi)/2$, the full solution of Eq. (4.12) with such a right-hand side can be written as

$$g_{f0} = (3/4) i e^{i\Phi} (\cos 2\Phi)^{-1/2} \int e^{-i\Phi} (\cos 2\Phi)^{1/2} d\Phi; \quad (5.1a)$$

$$g_2 = -i e^{-3i\Phi} (\cos 2\Phi)^{3/2} \int e^{3i\Phi} (\cos 2\Phi)^{1/2} d\Phi. \quad (5.1b)$$

Evaluating integrals in Eq. (5.1), we obtain:

$$g_{f0} = (3/8) [s(\Phi) e^{i\Phi} - 1]; \quad (5.2)$$

$$g_2 = -(1/4) \cos^2 2\Phi [s(\Phi) e^{-3i\Phi} + 1],$$

where

$$s(\Phi) \equiv [\ln(\sqrt{2} \cos \Phi + \sqrt{\cos 2\Phi}) \\ + i[\pi/2 + \sin^{-1}(\sqrt{2} \sin \Phi)]] (2 \cos 2\Phi)^{-1/2} \quad (5.3)$$

and the dependence on ξ can be recovered by recalling that $\tan 2\Phi = \xi$ and thus

$$\cos 2\Phi = (1 + \xi^2)^{-1/2}; \quad \cos^2 \Phi = (1 + \cos 2\Phi)/2.$$

The integration constants in Eq. (5.2) are chosen in such a way that P_{00} and P_{22} , Eq. (4.18), vanish as $\xi \rightarrow -\infty$. Figure 2 depicts the spatial dynamics of the mode component normalized powers P_{00} and P_{22} (as well as the total normalized SHG power, $P_{\text{SHG}} = P_{00} + P_{22}$), calculated by using Eqs. (5.2) and (4.18) as functions of the point of observation ξ . All of them have similar asymptotics at $\xi \rightarrow -\infty$, $P_{jj} = 0(\xi^{-3})$. The amplitudes’ asymptotics at $\xi \rightarrow \infty$ is as

$$|g_{f0}|^2 = \xi [2(3\pi/16)^2 + o(\xi^{-1})]; \quad (5.4)$$

$$|g_2|^2 = (\pi^2/32) \xi^{-3} + o(\xi^{-3}).$$

One can see from Fig. 2 that the main SHG transformation occurs within the focal area, after passing a few diffraction lengths, with the P_{SHG} steadily increasing. As $\xi \rightarrow \infty$, the SHG power reaches steady state, with the zeroth-order Gaussian mode strongly dominating, $P_{00} \gg P_{22}$:

$$P_{22}(\infty) = (\pi/16)^2; \quad P_{00}(\infty) = 18P_{22}(\infty); \\ P_{\text{SHG}}(\infty) = 19P_{22}(\infty) \approx 0.7325. \quad (5.5)$$

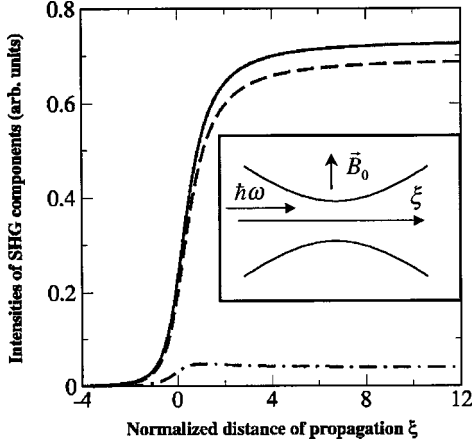


FIG. 2. Spatial dynamics of the SHG Gaussian mode components in the uniform dc magnetic field. Power of the zeroth-order P_{00} and second-order P_{22} components and the total normalized SHG power $P_{\text{SHG}} = P_{00} + P_{22}$ vs the normalized propagation distance $\xi \equiv y/y_d$. Curves: dash-dotted lines: P_{00} , dashed lines: P_{22} , solid lines: P_{SHG} . Inset: propagation configuration; a Gaussian beam at the fundamental frequency, with the beam normalized size $\delta = z/y_d$, propagates in the ξ axis; the dc magnetic field B_0 is normal to ξ .

Using Eq. (4.15), we can evaluate now the efficiency of the SHG conversion, $w_{\text{SHG}}(\infty)$, as

$$W_{\text{SHG}}(\infty) \equiv W_{\text{SHG}}(\infty)/W_1 = \sqrt{2\pi}(W_1/cz_0)P_{\text{SHG}}(\infty) \times (4\chi B_0)^2, \quad (5.6)$$

or, using Eq. (4.16) for W_1 , and Eq. (5.5) for $P_{\text{SHG}}(\infty)$, as

$$W_{\text{SHG}}(\infty) = \frac{19}{16\sqrt{2}} \left(\frac{\alpha}{45}\right)^2 \left(\frac{E_1 B_0}{B_{\text{cr}}^2}\right)^2 \approx 2.2 \times 10^{-8} \left(\frac{E_1 B_0}{B_{\text{cr}}^2}\right)^2. \quad (5.7)$$

Since $P_{\text{SHG}}(\infty)$ is a constant independent of any parameter of the problem, one can see from Eq. (5.6) that for the fixed laser power W_1 and the dc magnetic field B_0 the total output SHG power W_{SHG} is inversely proportional to the focal spot size z_0 . Thus, the effect increases with tighter focusing (and vanishes for plane wave) which is perfectly expected by now. On the other hand, the efficiency $w_{\text{SHG}}(\infty)$, Eq. (5.7), for the *fixed* field E_1 does *not* depend on the nonuniformity of the driving field (e.g., on the focal size z_0 or diffraction length y_d). Of course, this does not suggest the feasibility of SHG in a *plane wave*; one must note that Eq. (5.7) implies that the propagation length L is much larger than diffraction length y_d . However, as $z_0 \rightarrow \infty$ and $y_d \rightarrow \infty$, for any fixed (finite) L , one has $L \ll y_d$; using the exact solution in the form of Eqs. (5.1) and (5.2) (with new integration constant corresponding to P_{SHG} vanishing now at finite y) and evaluating the output field at finite distance $y=L$, one can readily show that $W_{\text{SHG}}(L/y_d \rightarrow 0)/W_1 \rightarrow 0$. Indeed, using in Eq. (5.1) the fact that $|\Phi| \ll 1$, $|\xi| \ll 1$, and $\Phi \approx \xi/2$, we obtain

$$g_{f0} \approx (3i/8)\xi + C_0; \quad g_2 \approx -(i/2)\xi + C_2; \quad (5.8)$$

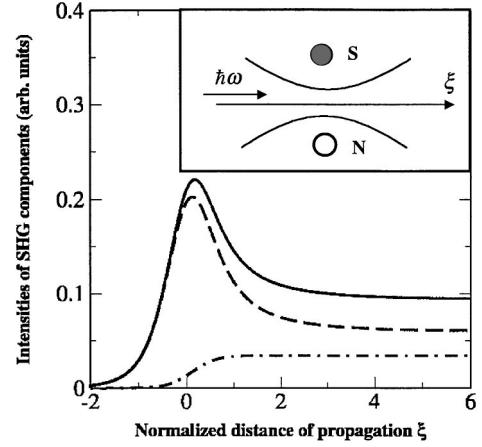


FIG. 3. The SHG spatial dynamics in the dc magnetic dipole in the case $z_B = y_d$ ($\delta_B = 1$). Curves and designation—same as in Fig. 2. Inset: propagation configuration with the magnetic dipole (two magnetic wires shown by hollow N and darkened S circles).

where C_0 and C_2 are integration constants. This yields that for the *finite* propagation length L ($\ll y_d$), in a dc magnetic field, the efficiency of the SHG conversion, $w_{\text{SHG}}(L)$, is

$$W_{\text{SHG}}(L) \equiv \frac{W_{\text{SHG}}(L)}{W_1} = \frac{11}{4\pi^2\sqrt{2}} \left(\frac{\alpha}{45}\right)^2 \left(\frac{E_1 B_0}{B_{\text{cr}}^2}\right)^2 \left(\frac{L}{y_d}\right)^2 = \frac{11W_{\text{SHG}}(\infty)}{19} \left(\frac{2L}{\pi y_d}\right)^2 \quad (5.9)$$

i.e., $w_{\text{SHG}}(L) \rightarrow 0$ as $y_d \rightarrow \infty$ as expected.

VI. A GAUSSIAN BEAM IN A dc MAGNETIC DIPOLE AND QUADRUPOLE

To study the gradient-induced SHG in a *nonuniform* magnetic field, we consider first a magnetic field originated by a 2D magnetic dipole, i.e., two thin parallel “magnetic” wires [17]. We will assume them located at the focal point of the fundamental Gaussian beam, positioned in the plane orthogonal to the beam (and extended, e.g., along the x axis), and spaced by $2z_B$ ($\gg z_0$) with the laser beam crossing the wire plane exactly in the middle of the structure, see inset in Fig. 3. The magnetic field of such a 2D dipole is

$$B_x = 0; \quad B_y = B_0 z_B y (l_+^{-2} - l_-^{-2})/2, \quad (6.1)$$

$$B_z = B_0 z_B [(z_B + z)l_+^{-2} + (z_B - z)l_-^{-2}]/2,$$

where B_0 is the maximum dc field (i.e., the field at the origin $y=z=0$) and $l_{\pm}^2 = y^2 + (z_B \pm z)^2$. (The same field is originated by a pair of cylinders of *finite* radius r_C , in which case $z_B = \sqrt{z_C^2 - r_C^2}$, where z_C is the distance between centers of the cylinders.) Since due to the condition $2z_B \gg z_0$, we can assume $B_z \gg B_y$, and since near the center of the beam, the longitudinal component of the dc field B_y , does not affect SHG anyway, the only dc component of consequence, as was shown in Sec. IV, is the transverse dc component, which, in the plane of symmetry ($z=0$), is

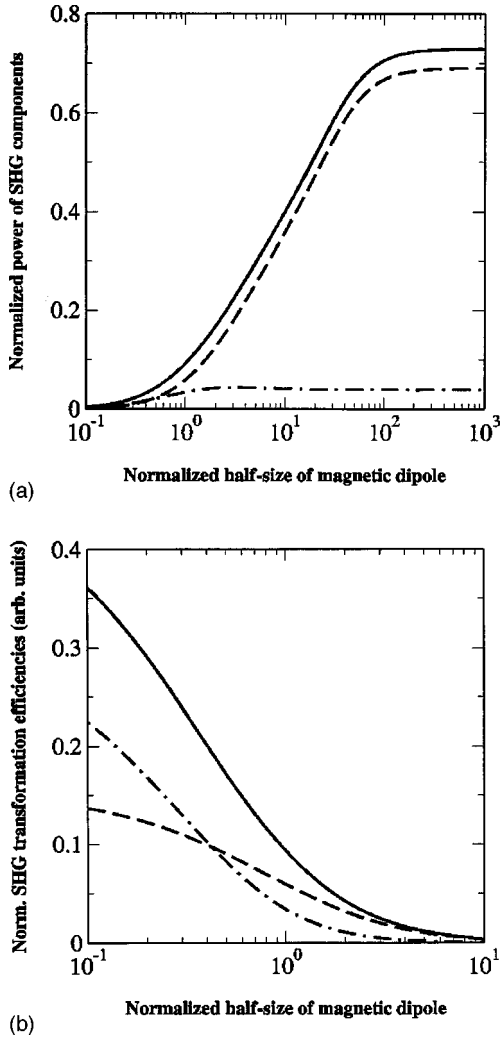


FIG. 4. (a) The output (power in the far-field area) of SHG, due to the dc magnetic dipole for the individual modes P_{00} and P_{22} and the total power P_{SHG} vs the normalized half-size of the dipole (i.e., half-spacing between wires) $\delta_B = z_B/y_d$; the maximal dc magnetic field is maintained constant B_0 , same as in Figs. 2 and 3. (b) The same for the normalized efficiencies ρ_{00} , ρ_{22} , and ρ_{SHG} , when the magnetic “charge” of each wire is retained constant as δ_B varies.

$$B_z(y) = B_0(1 + y^2/z_B^2)^{-1}, \quad (\text{with } B_y = 0, \quad B_x = 0). \quad (6.2)$$

Using again Eq. (4.12) with

$$\beta = (1 + \xi^2/\delta_B^2)^{-1}, \quad \text{where } \delta_B \equiv z_B/y_d; \quad (6.3)$$

and following the same procedure as in Eqs. (5.1) and (5.2), one can obtain analytic solution of Eq. (4.12) for both the zeroth-order (g_{0f}) and second-order (g_2) SHG Gaussian components in closed form. Without writing them here in explicit form, we depict their behavior in Figs. 3 and 4. The normalized power of these components, P_{00} and P_{22} (4.18), respectively, as well as the total normalized SHG power $P_{\text{SHG}} = P_{00} + P_{22}$ vs the normalized propagation distance, $\xi = y/y_d$, is shown in Fig. 3, where $\xi = 0$ corresponds to the

focal point, which is also the position of magnetic dipole, in the case $z_B = y_d$ ($\delta_B = 1$). For the sake of comparison with the data for *uniform dc* magnetic field, one is to remember that the absolute output SHG power W_{SHG} , see Eq. (4.15), is proportional to B_0^2 . Therefore, the output for absolute powers W_{00} , W_{22} , and W_{SHG} , using Fig. 3, can be directly related to the respective data for a *uniform dc* magnetic field (see the previous Section), if the magnetic dipole is chosen in such a way, that the maximum dc field, B_0 (i.e., here, the field at the point of origin $\xi = \zeta = 0$), is the same as for the reference uniform field. The most notable feature of the dc magnetic-dipole induced SHG, as seen in Fig. 3, is a large peak of the SHG power near the dipole position, the significant part of which, however, is converted back into fundamental frequency as the laser beam propagates. The peak sharpens (and its intensity increases) as the spacing between wires in the magnetic dipole decreases. In principle, this feature can be used to enhance the SHG output signal or directly measure it at the focal point, although the experimental realization of such measurements may prove to be difficult.

The transition from a dipole to a uniform field corresponds to the limit $\delta_B \rightarrow \infty$ (provided that the dc field B_0 at the focal point for both of these configurations is fixed). The gradual increase of the normalized output power of both the SHG component and total SHG power in the far-field area (i.e., for $y \gg y_d$ or $\xi \gg 1$) is shown in Fig. 4(a); one can see that they indeed approach the respective values for the uniform dc field.

Note that the behavior of the normalized powers P_{ij} does *not* depend on the magnitude B_0 . Thus, to analyze the dependence on B_0 , one needs to look at the absolute total power W , Eq. (4.15), or the efficiency of the SHG conversion w Eq. (5.6). If instead of maintaining the maximum dc field B_0 constant, the magnetic “charge” of each wire is retained constant (which amounts to $B_0 z_B = \text{const}$), the absolute power W Eq. (4.15) of both the SHG components and the total SHG power in the far-field area increases as the dipole half-size z_B *decreases*. This behavior is depicted in Fig. 4(b) where we show the normalized “efficiencies”

$$\rho_{00} = P_{00}/\xi^2, \quad \rho_{22} = P_{22}/\xi^2, \quad \rho_{\text{SHG}} = P_{\text{SHG}}/\xi^2,$$

vs ξ . This corresponds to the choice of the reference magnitude B_0 of the dc field to be that of the dipole with the $z_B = y_d$.

Another interesting feature of the dipole-induced SHG is that, while the zeroth-order SHG component dominates over the second-order component in the uniform dc field-induced SHG, Eq. (5.5), the ratio between these two components can be *controlled* by the size of the dc dipole. In particular, the powers of these two components equates when $\delta_B \approx 0.43$ [see Fig. 4(b)], and the second-order component becomes dominant for smaller δ_B .

To illustrate the evolution of the SHG spatial dynamics (in particular, large peaks formation) as the nonuniformity of the dc magnetic field becomes more complicated, we consider a dc magnetic *quadrupole*, which consists of four magnetic wires forming e.g., square (Fig. 5), with the spacing between any pair of adjacent wires being $2z_B (= 2\delta_B y_d)$. In

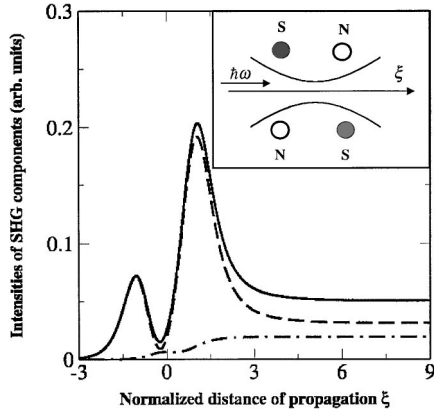


FIG. 5. The SHG spatial dynamics in the dc magnetic quadrupole in the case $\delta_B=1$. Curves and designation—same as in Figs. 2 and 3. Inset: propagation configuration with the magnetic quadrupole (four magnetic wires).

this case, the normalized transverse component of the dc magnetic field in the plane of symmetry ($z=0$) in Eq. (4.12) is

$$\beta = [1 + (\xi/\delta_B + 1)^2]^{-1} - [1 + (\xi/\delta_B - 1)^2]^{-1} \quad (6.4)$$

with the dc field vanishing at the origin; $\beta=0$ at $\xi=\zeta=0$. The power of zeroth- and second-order Gaussian components, P_{00} and P_{22} , Eq. (4.18), respectively, as well as $P_{\text{SHG}}=P_{00}+P_{22}$, vs the normalized propagation distance, $\xi=y/y_d$, is shown in Fig. 5, where $\xi=0$ corresponds to the focal point, which is also the center of magnetic quadrupole, in the case $z_B=y_d$ ($\delta_B=1$). One can see pronounced large peaks in the vicinity of each of the dipoles forming the quadrupole. However, a considerable SHG can still be observed in the far-field area.

VII. DISCUSSION OF THE RESULTS

This paper does not pursue specific experimental design or optimization calculations for the SHG effect in magnetized vacuum. Next step to such a design is to calculate 3D cw (i.e., cylindric) Gaussian beam propagation in a dc magnetic field (compare with 2D Gaussian beam, see here Sec. IV–VI), and combine it, in the general case, with temporal effect in a laser pulse (see Sec. III). However, to get the idea of expected effect, we can have an order-of-magnitude estimate using the results obtained here. First, we note that in the conventional sources (lasers), the spatial compression (focusing) of laser beams is much stronger than temporal compression (i.e., $z_0/\lambda = O(1) \ll t_p \omega/2\pi$). Most recently, there were quite a few proposals to achieve a single-cycle or subcycle subfemtosecond pulses [21], but even when experimentally obtained, they will have too broad a spectrum and may not be optimal for the first observation of a coherent SHG. Thus at this point, to be on conservative side, we neglect temporal effects and consider only spatial effects. Total SHG photon output, Φ_{SHG} , is

$$\begin{aligned} \Phi_{\text{SHG}}(s^{-1}) &= \bar{\rho}_1 w_{\text{SHG}}/2\hbar\omega \\ &\approx 1.2 \times 10^{-38} \bar{\rho}_1 (\text{W}) I_1 (\text{W/cm}^2) \lambda (\mu\text{m}) B_0^2 (\text{ts}), \end{aligned} \quad (7.1)$$

where $\bar{\rho}_1$ is the total time-averaged power of fundamental harmonics (in W), λ is the wavelength of fundamental harmonics (in μm), I_1 is the maximal intensity of fundamental harmonics (in W/cm^2) at focal point, and magnetic field B_0 is in Tesla. Rapid advent of laser and magnet technologies makes the observation of vacuum SHG feasible in the near future. Let us consider, for example, a laser with $\lambda \approx 0.8 \mu\text{m}$ (as in Ti-Spph laser), with $\bar{\rho}_1 \sim 10^5 \text{ W}$ and intensity at focal point $I_1 \sim 10^{22} \text{ W/cm}^2$ (both of which constitute about two orders of improvement to the best existing lasers), and $B_0 \sim 10^3 \text{ ts}$ (which can currently be obtained by explosions). Equation (7.1) yields then ~ 85 photons/day.

An apparent interpretation of nonvanishing SHG is that the nonuniformity allows for the momentum transfer between photons and dc field (which would ultimately result in the recoil of material system generating the dc field), thus breaking the symmetry that causes vanishing interaction of a completely uniform field system. This explanation could be directly corroborated by e.g., direct QED calculations of SHG by two collinear photons+elementary source (particle) of the dc field, similarly to quasielastic scattering of a *single* photon at a Coulomb potential [22], see also Refs. [2,18,19] (QED calculations of photon splitting probability in a nucleus Coulomb potential using the recoil momentum can be found in Ref. [23]). Examples of such sources could be protons (or heavy nuclei) or neutrons with two collinear photons “SHG scattered” at the particle spin and Coulomb dc (electric) field. In macroscopic terms, the paraxial approximation for SHG, Eq. (2.10), is not valid here, and SHG is originated by an elementary multipole source, Eq. (2.7), in a limited volume $\ll \lambda_1^3$ (similarly to Sec. V in Ref. [6]); we found that in the lowest approximation, the source is a dipole for a spin and a quadrupole for a Coulomb field.

All the calculations in this paper were based on the QED box approximation involving only the term L_4 . Let us roughly estimate the order of magnitude of the next, hexagonal term L_6 . Using the approach of Refs. [1,2], L_6 was evaluated by us as:

$$L_6 = \gamma a(b^2/2 + a^2/13) \quad \text{with} \quad \gamma = (26/315) \alpha / \pi B_{\text{cr}}^4, \quad (7.2)$$

where a and b are the same as in Eqs. (1.1) and (2.4), it results in the nonlinear terms [17]:

$$\vec{D}^{NL} = \gamma [(b^2 + 6a^2/13) \vec{E} + ab \vec{B}], \quad (7.3a)$$

$$\vec{H}^{NL} = \gamma [-(b^2 + 6a^2/13) \vec{B} + ab \vec{E}] \quad (7.3b)$$

[compare with Eq. (2.4)]. To fully compare box and hexagonal term contributions, one has to solve the propagation configurations (considered here for L_4) for L_6 now, which is far beyond the scope of this paper. A very rough estimate, however, can be made presuming that inhomogeneity plays the

same role in both L_6 and L_4 approximations, in which case the ratio between the respective SHG outputs can be estimated as

$$(W_{\text{SHG}})_{\text{hex}}/(W_{\text{SHG}})_{\text{box}} = O(\max(E_1^4, B_0^4)/B_{\text{cr}}^4). \quad (7.4)$$

For the highest currently available laser and dc fields, this ratio is $\sim 10^{-18} - 10^{-16}$. Even for the example considered in the beginning of this section, this ratio is $\sim 10^{-12}$. Thus, the hexagonal term makes a negligible contribution to SHG for any fields accessible in the laboratory now and in the foreseeable future.

VIII. CONCLUSION

In conclusion, we demonstrated the feasibility of field-gradient-induced second-harmonic generation (SHG) by the

intense laser radiation in a dc magnetic field in a vacuum; the SHG effect does not vanish in the QED box diagram approximation only if the participating fields are temporarily/spatially nonuniform.

ACKNOWLEDGMENTS

We are indebted to M. G. Raizen, B. Rosenstein, G. W. Ford, and D. G. Steel, whose critical and valuable comments and ensuing discussions provided an essential momentum for us to undertake this research. One of us (A.E.K.) thanks P. L. Shkolnikov and I. Bialynicki-Birula for interesting discussions and Dmitri Bitouk for his help with the figures. The work of A.E.K. is supported by the U.S. Air Force Office of Scientific Research.

-
- [1] H. Euler, *Ann. Phys. (Leipzig)* **26**, 398 (1936); W. Heisenberg and H. Euler, *Z. Phys.* **98**, 714 (1936); V. Weisskopf, *Kgl. Danske Videnskab. Selskabs. Mat.-fys. Medd.* **14** (6) (1936).
 - [2] A. I. Akhiezer and V. B. Berestetskii, *Quantum Electrodynamics* (Interscience, New York, 1965), pp. 764–792.
 - [3] Z. Bialynicka-Birula and I. Bialynicki-Birula, *Phys. Rev. D* **2**, 2341 (1970); I. Bialynicki-Birula and Z. Bialynicka-Birula, *Quantum Electrodynamics* (Pergamon & Polish, Warszawa, 1975).
 - [4] E. B. Aleksandrov, A. A. Ansol'm, and A. N. Moskalev, *Zh. Eksp. Teor. Fiz.* **89**, 1181 (1985) [*Sov. Phys. JETP* **62**, 680 (1985)].
 - [5] R. L. Dewar, *Phys. Rev. A* **10**, 2107 (1974).
 - [6] J. McKenna and P. M. Platzman, *Phys. Rev.* **129**, 2354 (1963).
 - [7] Z. Bialynicka-Birula, *Acta Phys. Pol. A* **57**, 729 (1980); *Phys. Rev. D* **2**, 513 (1981).
 - [8] (a) S. L. Adler, J. N. Bahcall, C. G. Callan, and M. N. Rosenbluth, *Phys. Rev. Lett.* **25**, 1061 (1970); (b) S. L. Adler, *Ann. Phys. (N.Y.)* **67**, 599 (1971).
 - [9] D. V. Gal'tsov and V. V. Skobelev, *Zh. Eksp. Teor. Fiz.* **13**, 173 (1971) [*JETP Lett.* **13**, 122 (1971)].
 - [10] V. G. Skobov, *Zh. Eksp. Teor. Fiz.* **35**, 1315 (1958) [*Sov. Phys. JETP* **8**, 919 (1959)]; A. Minguzzi, *Nuovo Cimento* **19**, 847 (1961); T. Erber, *Rev. Mod. Phys.* **38**, 626 (1966).
 - [11] S. S. Sannikov, *Zh. Eksp. Teor. Fiz.* **52**, 1303, (1967) [*Sov. Phys. JETP* **25**, 867 (1967)].
 - [12] R. J. Stoneham, *J. Phys. A* **12**, 2187 (1979).
 - [13] Y. J. Ding and A. E. Kaplan, *Phys. Rev. Lett.* **63**, 2725 (1989).
 - [14] M. G. Raizen and B. Rosenstein, *Phys. Rev. Lett.* **65**, 2744 (1990).
 - [15] G. W. Ford and D. G. Steel, *Phys. Rev. Lett.* **65**, 2745 (1990).
 - [16] Y. J. Ding and A. E. Kaplan, *Phys. Rev. Lett.* **65**, 2746 (1990).
 - [17] Y. J. Ding and A. E. Kaplan, *Int. J. Nonlinear Opt. Phys.* **1**, 51 (1992).
 - [18] V. B. Berestetskii, E. M. Lifshitz, and L. P. Pitaevskii, *Quantum Electrodynamics* (Pergamon Press, New York, 1982), Section 129, pp. 575–585.
 - [19] J. Schwinger, *Phys. Rev.* **82**, 664 (1951); in *Particles, Sources, and Fields*, (Addison-Wesley, NY, 1989), Vol. II, Sec. 4-8.
 - [20] K. Miyazaki, T. Sato, and K. Kashiwagi, *Phys. Rev. A* **23**, 1358 (1981); D. S. Bethune, *ibid.* **23**, 3139 (1981); L. Marmet, K. Hakuta, and B. P. Stoicheff, *JOSA B* **9**, 1038 (1992).
 - [21] T. W. Hansch, *Opt. Commun.* **80**, 71 (1990); G. Farkas and C. Toth, *Phys. Lett. A* **168**, 447 (1992); A. E. Kaplan, *Phys. Rev. Lett.* **73**, 1243 (1994); P. B. Corkum, N. H. Burnett, and M. Y. Ivanov, *Opt. Lett.* **19**, 1870 (1994); A. E. Kaplan and P. L. Shkolnikov, *Phys. Rev. Lett.* **75**, 2316 (1995); *JOSA B* **13**, 347 (1996); A. E. Kaplan, S. F. Straub, and P. L. Shkolnikov, *Opt. Lett.* **22**, 405 (1997); *JOSA B* **14**, 3013 (1997); I. P. Christov, M. M. Murnane, and H. C. Kapteyn, *Phys. Rev. Lett.* **78**, 1251 (1997); S. E. Harris and A. V. Sokolov, *ibid.* **81**, 2894 (1998); A. Nazarkin and G. Korn, *ibid.* **83**, 4748 (1999); A. V. Sokolov, D. D. Yavuz, and S. E. Harris, *Opt. Lett.* **24**, 557 (1999).
 - [22] M. Delbrück, *Z. Phys.* **84**, 144 (1933); F. Röhrlich and R. L. Gluckstern, *Phys. Rev.* **86**, 1 (1952); R. R. Wilson, *ibid.* **90**, 720 (1953).
 - [23] Y. Shima, *Phys. Rev.* **142**, 944 (1966); A. M. Johannessen, K. J. Mork, and I. Overbo, *Phys. Rev. D* **22**, 1051 (1980).